Supplementary Materials for

Stimulation of *de novo* pyrimidine synthesis by growth signaling through mTOR and S6K1

Issam Ben-Sahra[1†], Jessica J. Howell[1†], John M. Asara[2], Brendan D. Manning[1*]

†These authors contributed equally to this work.

correspondence to: bmanning@hsph.harvard.edu

This PDF file includes:

Other Suplementary Materials for this manuscript includes the following:
(URL for Table S1**)**

Table S1. LC/MS/MS peak areas and *P*-values for experiments described in Fig. 1A-C (ranked by *P*-values of pairwise comparisons)

Materials and Methods

Antibodies, growth factors, inhibitors, isotopic tracers, and other reagents

Reagents were obtained from the following sources. Antibodies to phospho- (P-)S6K1-T389 (CST#9234), P-S6-S240/S244 (CST#2215), P-Ser motif (P-(Ser) 14-3-3-Binding Motif Antibody, CST#9601), P-Rictor-T1135 (CST#3806), S6K1 (CST#2708), S6 (CST#2217), P-p90RSK-S380 (CST#9335), HA (CST#3724, for immunoblots), and HRP-labeled anti-mouse and anti-rabbit secondary antibodies were from Cell Signaling Technology. CAD antibodies were from Origene (TA303410, for human cells), P-CAD-T456 from Santa Cruz (sc-12964-R), and anti-sera provided by Cell Signaling Technology for total and P-CAD-S1859 (antibodies under development). Antibodies to DHODH from Protein Tech, Rictor from Bethyl (A300-459A), and β-actin from Sigma. For immunoprecipitations, HA antibody from Covance (MMS-101P) and anti-FLAG M2 Affinity Gel from Sigma were used.

Insulin, G418, L-glutamine, D-Glucose, ^{15}N-glutamine-amide, and ^{13}C-4-aspartic acid were from Sigma-Aldrich. 1,2-^{3}H-2-deoxy-D-Glucose, U^{14}C-glutamine, U^{14}C-aspartic acid, 5,6-^{3}H-uridine, and 6-^{3}H-thymidine were from Perkin-Elmer. EGF (human recombinant) was from Peprotech. SuperScript III kit, Lipofectamine 2000, Lipofectamine RNAi max, Lipofectamine LTX, and glucose-free DMEM were from Invitrogen. Glutamine-free DMEM was from Lonza. DMEM, DMEM/F12 were from CellGro, Ham's F-12K from ATCC, Ham's F-12 and glutamine-free F-12 from Sigma, and amino acid-free DMEM from Gibco. Fetal bovine serum (FBS) and protease inhibitor cocktail were from Sigma. Chemical inhibitors include rapamycin from LC Laboratories, PF-4708671 (S6K1i) from Tocris Biosciences, and A771726 and U0126 from EMD Millipore Bioscience. Bradford assay reagent from Bio-Rad, protein A/G agarose from Pierce; Allprep DNA/RNA mini kit and RNeasy from Qiagen, Phusion® High-Fidelity DNA Polymerase was from New England Biolabs; siRNAs were from Dhamacon (ON-TARGETplus SMARTpool); *Power* SYBR® Green PCR Master Mix used for qPCR was from Applied Biosystems.

Cell lines and tissue culture

MEFs, HeLa, U87MG-iPTEN and 293Es were cultured in DMEM with 10% FBS, 37°C, 5% CO_2. *Tsc2*$^{+/+}$ *p53*$^{-/-}$ and *Tsc2*$^{-/-}$ *p53*$^{-/-}$ MEFs were provided by David Kwiatkowski (Harvard Medical School). U87MG-iPTEN were cultured in presence of Neomycin (0.4 mg/ml) and were developed in the laboratory of Maria-Magdalena Georgescu (MD Anderson Cancer Center). MCF10A were cultured in DMEM F12 with 5% Horse serum, EGF (20ng/ml), Hydrocortisone (0.5mg/ml), Cholera Toxin (100ng/ml), Insulin (10μg/ml) and Penicillin/Streptomycin (1mM), 37°C, 5% CO_2, with pools stably expressing K-Ras^{G12V} or PI3KCA^{H1047R}, via retroviral infection with pBabe-Puro constructs and subsequent selection, also cultured in presence of puromycin (0.5 μg/ml). The Cho-K1-derived CAD-deficient cell line (G9C) was kindly provided by David Patterson (University of Denver) and were cultured in F-12K media supplemented with 10% FBS, 30-μM uridine, and 1-mM Penicillin/Streptomycin. G9C cells stably transfected with vector or FLAG-HA-CAD (WT or S1859A) were maintained in media

supplemented with 500 μg/mL G418. Media was changed to Ham's F-12 without uridine 24h prior to labeling and metabolite extraction.

Viable cell counts were obtained using a MOXI-Z Mini Cell Counter from Orflo. Cell cycle analyses were performed by flow cytometry (FACSCalibur, Bectin Dickinson) following 15-h fixation at -20ºC in 75% ethanol and 2-h incubation in propidium iodide solution (3.8 mM sodium citrate, 40 μg/ml propidium iodide, 10 μg/ml RNASE A) in the dark at 4 ºC.

Constructs and transfections

Full-length murine CAD was cloned from 3T3-L1 cell cDNA into a pcDNA3 vector containing the FLAG-HA-tag. The S1859A and S1900A mutations were generated by Dpn I-mediated site-directed mutagenesis using Phusion High-Fidelity DNA Polymerase. All clones were completely sequenced to verify the lack of additional mutations. 10-cm dishes of near confluent HEK-293E cells were transfected using Lipofectamine 2000, according to the manufacturer's instructions, with 10 μg of plasmid DNA; cells were split 8 h post-transfection for the experiments described. For co-transfection of siRNA and plasmid DNA, 6 μg of DNA and 300 pmol of siRNA (23 nM final concentration) were combined and transfected with Lipofectamine 2000. For G9C cells, 18 μg of plasmid DNA was transfected into 10-cm dishes at 90% confluence using the Lipofectamine LTX reagent at a ratio of 3.5:1. 16 h post-transfection, cells were cultured onto new 10-cm plates at 1.5 x 10^6 cells, allowed to recover for 48 h, serum starved for 16 h and treated as described. For all other siRNA experiments, siRNAs (On TARGETplus SMARTpool, Dharmacon) were used at 32 nM (final concentration) with 5 μL of Lipofectamine RNAimax (6-well) or 20 μL of Lipofectamine RNAimax (10-cm plate) for each condition**.**

Immunoprecipitation and immunoblotting

Cells were lysed in ice-cold NP-40 lysis buffer (40 mM HEPES, pH 7.4, 120 mM NaCl, 1 mM EDTA, 1% NP-40 [Igepal CA-630], 5% glycerol, 10 mM sodium pyrophosphate, 10 mM glycerol 2-phosphate, 50 mM NaF, and 0.5 mM sodium orthovanadate) and incubated on ice for 15 min. Lysates were centrifuged at 16,000 x *g* for 15 min at 4°C. Protein concentrations were measured by Bradford assay and normalized, separated by SDS-PAGE, and transferred onto PVDF membranes for immunoblotting (Immobilon-P, Millipore). Membranes were blocked in 5% Milk in 0.1% TBS-Tween, and incubated overnight at 4°C with the indicated antibodies. FLAG-HA-tagged CAD and HA-S6K1 were immunoprecipitated from cell lysates by incubation with either FLAG-M2 agarose or HA antibody for 2-3 hours, rotating, at 4°C. For HA immunoprecipitations, Protein A/G agarose was added to the incubation mixture for an additional 1-2 hours. Beads were washed in NP-40 buffer and resuspended in Laemmli buffer, or, for mass spectrometric analysis, eluted from the beads by further incubation with 200 μg/mL 3xFLAG peptide (Sigma) in TBS on ice for 1h.

In vitro kinase assay

HEK 293E cells were plated at $3x10^6$ per 10-cm dish, one day prior to transfection. Cells were transfected with empty vector (pcDNA3-FLAG), FLAG-HA-CAD or FLAG-HA-CAD-S1859A, or empty vector (pRK7), HA-S6K1 or HA-S6K1-KD (kinase dead), and approximately 24 hours post-transfection, were split onto 15-cm plates. FLAG-HA-CAD was immunoprecipitated with an HA antibody from lysates of serum-starved cells that had been treated with rapamycin for 1h prior to lysis to block phosphorylation by endogenous rapamycin-sensitive kinases. HA-S6K1 was immunoprecipitated with an HA antibody from lysates of cells that were serum starved and stimulated with 100 nM insulin for 1h prior to lysis. HA-S6K1-containing immune complexes were precipitated using protein A/G agarose beads with the CAD substrate already bound. Following three washes in lysis buffer, the beads containing both substrate and kinase were washed twice in S6K1 kinase reaction buffer (20 mM HEPES, 10 mM MgCl2, 0.5 mM EGTA, pH 7.4), and kinase reactions were carried out in 15 μL of reaction buffer containing 100 μM ATP and 10 mM dithiothreitol at 32°C for 20 min. Reactions were stopped by boiling the mixtures in SDS sample buffer and analyzed by immunoblotting.

Phospho-peptide analysis of CAD by mass spectrometry

For mass spectrometry (MS) experiments, FLAG-HA-CAD immunoprecipitates were eluted with 3xFLAG peptide and separated by SDS-PAGE, the gel was stained with Coomassie blue, and the CAD band was excised. Gel slices were subjected to reduction with dithiothreitol, alkylation with iodoacetamide, and in-gel digestion with chymotrypsin overnight at pH 8.3, followed by reversed-phase microcapillary/tandem mass spectrometry (LC-MS/MS). LC-MS/MS was performed using an Easy-nLC nanoflow HPLC (Thermo Fisher Scientific) with a self-packed 75 mm id x 15 cm C_{18} column connected to a hybrid linear ion trap LTQ-Orbitrap XL mass spectrometer (Thermo Fisher Scientific) in the data-dependent acquisition and positive ion mode at 300 nL/min. MS/MS spectra collected via collision induced dissociation in the ion trap were searched against the concatenated target and decoy (reversed) Swiss-Prot and FLAG-CAD single entry protein databases using Sequest with differential modifications for Ser/Thr/Tyr phosphorylation (+79.97) and the sample processing artifacts Met oxidation (+15.99), deamidation of Asn and Gln (+0.984) and Cys alkylation (+57.029) as affixed modification. Phosphorylated and unphosphorylated peptide sequences were identified if they initially passed the following Sequest scoring thresholds against the target database: 1+ ions, Xcorr ³ 2.0 Sf ³ 0.4, P ³ 5; 2+ ions, Xcorr ³ 2.0, Sf ³ 0.4, P ³ 5; 3+ ions, Xcorr ³ 2.60, Sf ³ 0.4, P ³ 5 against the target protein database. Passing MS/MS spectra were manually inspected to be sure that all b- and y- fragment ions aligned with the assigned sequence and modification sites. Determination of the exact sites of phosphorylation was aided using *FuzzyIons* and *GraphMod* software (Proteomics Browser Software suite, Harvard University). False discovery rates (FDR) of peptide hits were estimated below 1.2% based on reversed database hits.

Measurements of glucose and glutamine uptake

Glucose uptake was measured as the incorporation of radiolabeled 1,2-^{3}H-2-deoxy-D-glucose, based on a previously described method (*19*). Cells were grown in 12-well plates and serum starved in the presence of vehicle (DMSO), rapamycin, or PF-4708671 for 8 hours. Cells were then washed twice with preheated KRP buffer (10 mM $NaH2PO_4$/$Na2HPO_4$ pH 7.4, 136 mM NaCl, 4.7 mM KCl, 1.25 mM $MgSO_4$, 1.25 mM $CaCl_2$) containing 0.2% bovine serum albumin (BSA) and incubated for 15 min in 0.85 ml KRP/BSA, followed by addition of 0.1 mM cold 2-deoxy-D-glucose and 0.5 μCi 1,2-^{3}H-2-deoxy-D- glucose for 5 min. Cells were then placed on ice, washed twice with ice-cold PBS, and lysed in 0.5 ml of 1% NP40 lysis buffer. 0.4 ml lysate was counted in 5 ml of scintillation fluid using a Beckman LS6500 scintillation counter. The glucose uptake was normalized to protein concentration. Each cell line and condition was assayed in triplicate.

Glutamine was measure as the incorporation of radiolabeled U-^{14}C-glutamine. Cells were grown in 6-well plates and serum starved for 15 hours and treated with vehicle (DMSO) or 20 nM rapamycin for 1h. Cells were then washed twice with preheated KRP buffer containing 0.2% BSA and incubated for 15 min in 0.85 ml KRP/BSA, followed by addition of 1 mM cold L-glutamine and 1 μCi U-^{14}C-glutamine for 10 min. Cells were then placed on ice, washed twice with ice-cold PBS, and lysed in 0.5 ml of 1% NP40 lysis buffer. 0.4 ml lysate was counted in 5 ml of scintillation fluid using a Beckman LS6500 scintillation counter. The glutamine uptake was normalized to cell number. Each cell line and condition was assayed in triplicate.

Metabolite profiling for steady state and targeted flux analyses (Metabolomics)

To determine the relative levels of intracellular metabolites, extracts were prepared and analyzed by LC/MS/MS. Triplicate 10-cm plates (~80% confluent) were incubated in serum-free medium for 15 h, with a medium change 2 h prior to extraction. For ^{15}N-glutamine flux studies, cells were washed once with serum- and glutamine-free DMEM and then incubated in the same containing 5-mM ^{15}N-glutamine for 15 min. For [4-^{13}C]-aspartate flux studies, cells were washed once with serum free DMEM and then incubated in the same containing 4-mM ^{13}C-aspartic acid for 15 min. For D-[1,2-^{13}C]-glucose flux studies, cells were washed once with serum- and glucose free DMEM and then incubated in DMEM containing a 10-mM 1:1 mixture of D-[1,2-^{13}C]-glucose and unlabeled D-glucose for 15 min. Metabolites were extracted on dry ice with 4-mL 80% methanol (-80°C), as described previously (*4*). Insoluble material was pelleted by centrifugation at 3000*g* for 5 min, followed by two subsequent extractions of the insoluble pellet with 0.5-ml 80% methanol, with centrifugation at 16000*g* for 5 min. The 5-ml metabolite extract from the pooled supernatants was dried down under nitrogen gas using an N-EVAP (Organomation Associates, Inc).

Dried pellets were resuspended using 20 μL HPLC grade water for mass spectrometry. 10 μL were injected and analyzed using a 5500 QTRAP triple quadrupole mass spectrometer (AB/SCIEX) coupled to a Prominence UFLC HPLC system (Shimadzu) via selected reaction monitoring (SRM) of a total of 254 endogenous water soluble metabolites for steady-state analyses of samples (*20*). Some metabolites were targeted in

both positive and negative ion mode for a total of 287 SRM transitions using pos/neg polarity switching. ESI voltage was +4900V in positive ion mode and –4500V in negative ion mode. The dwell time was 3 ms per SRM transition and the total cycle time was 1.55 seconds. Approximately 10-14 data points were acquired per detected metabolite. Samples were delivered to the MS via normal phase chromatography using a 4.6 mm i.d x 10 cm Amide Xbridge HILIC column (Waters Corp.) at 350 µL/min. Gradients were run starting from 85% buffer B (HPLC grade acetonitrile) to 42% B from 0-5 minutes; 42% B to 0% B from 5-16 minutes; 0% B was held from 16-24 minutes; 0% B to 85% B from 24-25 minutes; 85% B was held for 7 minutes to re-equilibrate the column. Buffer A was comprised of 20 mM ammonium hydroxide/20 mM ammonium acetate (pH=9.0) in 95:5 water:acetonitrile. Peak areas from the total ion current for each metabolite SRM transition were integrated using MultiQuant v2.0 software (AB/SCIEX). For stable isotope labeling experiments, custom SRMs were created for expected ^{15}N or ^{13}C incorporation in various forms for targeted LC/MS/MS. The list of custom SRMs covering the pyrimidine synthesis and pentose phosphate pathways are provided in table S2. The methods are similar to those described previously (*21, 22*), but with short labeling times (15 min) to capture early flux events. Peak areas of metabolites detected by mass spectrometry were normalized to median and then normalized to protein concentrations. The values for each metabolite analyzed in the steady state metabolomic experiments from Fig 1A-C are provided in table S1.

U-^{14}C-aspartate incorporation into RNA, rRNA, and DNA

Cells were serum starved for 15 hours and treated as indicated in the figures. All conditions were in biological triplicates and treated with 2-µCi U-^{14}C-aspartate plus either 1 µCi 5,6-^{3}H-uridine (RNA) or 1 µCi 6-^{3}H-thymidine (DNA) for the indicated times. Cells were harvested and RNA or DNA was isolated using Allprep DNA/RNA kits according to the manufacturer's instructions and quantified using a spectrophotometer. Equal volumes of DNA or RNA were added to scintillation vials and radioactivity was measured by liquid scintillation counting and normalized to total DNA or RNA concentration, respectively.

For analysis of rRNA, cells were plated at 5×10^6 cells per 15-cm dish in the appropriate medium. At 70% confluence, cells were transfected with non-targeting siRNAs (siCtl) or siRNAs targeting S6K1. Cells were serum starved for 15 hours and stimulated or not with 100-nM insulin and incubated with 2-µCi U-^{14}C-aspartate plus 1-µCi 5,6-^{3}H-uridine for 6 hours. Cells were washed with cold D-PBS, pH 7.4 and scraped into 10 ml of D-PBS. Ribosomal RNA was isolated using a previously established protocol (*23*). Cells were collected by centrifugation at 500 *g* for 5 min at 4°C and resupended with cold Buffer A (250 mM sucrose, 250mM KCl, 5 mM $MgCl_2$, 50 mM Tris-HCl, pH 7.4). The cell suspension was lysed by adding NP-40 (final concentration of 0.7 %), and lysates were centrifuged 750 *g* for 10 min at 4°C to pellet and remove nuclei. The supernatant (cytosolic fraction) was centrifuged 12,500 g for 10 min at 4°C to discard mitochondria. The post-mitochondrial fraction (PMT), which contains ribosomes, was retained and KCl was added to a 0.5 M final concentration. For each sample, the volumes were adjusted using cold Buffer B (250 mM sucrose, 0.5 M KCl, 5 mM $MgCl_2$, 50 mM Tris-HCl, pH 7.4). Ribosome pellets were harvested by ultracentrifugation for 250,000 *g* for 3 hours at

4°C. The supernatants were discarded and ribosome pellets were resuspended with cold Buffer C (25 Mm KCl, 5 mM $MgCl_2$, 50 mM Tris-HCl, pH 7.4). Ribosomal RNA was purified using the RNA clean up method according to the RNeasy kit manufacturer's instruction. Ribosomal RNA concentrations were measured by spectrophotometer at 260 nm. 30 µL of ribosomal RNA was added to scintillation vials and radioactivity was measured by liquid scintillation counting and normalized to total ribosomal RNA concentration. In parallel, 1 µg of ribosomal RNA was loaded on a 1% agarose gel for visualization.

mRNA expression analysis

For quantification of *Cad* and *Dhodh* mRNA expression, total cellular RNA was isolated (RNeasy kit) from cells grown in the indicated conditions and reverse-transcription (SuperScript III kit) was performed. The resulting cDNA was diluted in DNase free water (1:40) before quantification by real-time PCR. Data are expressed as the ratio between *Cad* or *Dhodh* expression and β-*Actin* for human or *36B4* for mouse. The following primers were used for quantitative real-time PCR:

β-Actin (*Homo sapiens*)
Forward: AGAAAATCTGGCACCACACC
Reverse: GGGGTGTTGAAGGTCTCAAA

Cad (*Homo sapiens*)
Forward: AGTGGTGTTTCAAACCGGCAT
Reverse: CAGAGACCGAACTCATCCATTTC

Dhodh (*Homo sapiens*)
Forward: GTTCTGGGCCATAAATTCCGA
Reverse: CCTTCCTGAGGTTTTGGAGTC

36b4 (*Mus musculus*)
Forward: AGATGCAGCAGATCCGCAT
Reverse: GTTCTTGCCCATCAGCACC

Cad (*Mus musculus*)
Forward: CAACTACGGCATTCCCTCAGA
Reverse: GAGGATTCAAACCACTTGCTCA

Dhodh (*Mus musculus*)
Forward: TCTTCACCTCTTACCTGACAGC
Reverse: CATGTTGGAGTCCTGAAACGTA

Statistical analyses

MetaboAnalyst was used to assist data analyses (http://www.metaboanalyst.ca). For heat maps, normalized peak areas were sorted based on their Marker selection using GENE-E software from the Broad institute (http://www.broadinstitute.org/cancer/software/GENE-

E/). Marker selection identifies entities (e.g., metabolites) that are present at different levels between experimental conditions, and the software estimates the significance (*P*-value) of the differences, correcting for multiple hypotheses testing by calculating the false discovery rate and family-wise error rate. The normalized MS/MS peak values for each individual sample, as well as the average values, SD, and SEM for the 3 biological replicates, for all metabolites from the metabolomic profiles are provided in table S1 and ranked by *P*-value. Only those with $P<0.01$ are shown in the heat maps in Fig 1A-C. A two-tailed Student's t-test was performed for all pairwise comparisons ($N=3$). The distributions of the variables of interest are normal. All *P*-values for pairwise comparisons of metabolic flux data and radiolabeling of DNA and RNA from the main figures are provided in tables S3 and S4, with those having $P<0.05$ in supplemental figures being provided within the figure.

Supplemental references

4. K. Duvel *et al.*, Activation of a metabolic gene regulatory network downstream of mTOR complex 1. *Mol Cell* 39, 171 (Jul 30, 2010).
19. J. F. Tanti, M. Cormont, T. Gremeaux, Y. Le Marchand-Brustel, Assays of glucose entry, glucose transporter amount, and translocation. *Methods Mol Biol* 155, 157 (2001).
20. M. Yuan, S. B. Breitkopf, X. Yang, J. M. Asara, A positive/negative ion-switching, targeted mass spectrometry-based metabolomics platform for bodily fluids, cells, and fresh and fixed tissue. *Nature protocols* 7, 872 (May, 2012).
21. H. Ying *et al.*, Oncogenic Kras maintains pancreatic tumors through regulation of anabolic glucose metabolism. *Cell* 149, 656 (Apr 27, 2012).
22. J. W. Locasale *et al.*, Phosphoglycerate dehydrogenase diverts glycolytic flux and contributes to oncogenesis. *Nat Genet* 43, 869 (Sep, 2011).
23. S. Belin *et al.*, Purification of ribosomes from human cell lines. *Curr Protoc Cell Biol* Chapter 3, Unit 3 40 (Dec, 2010).

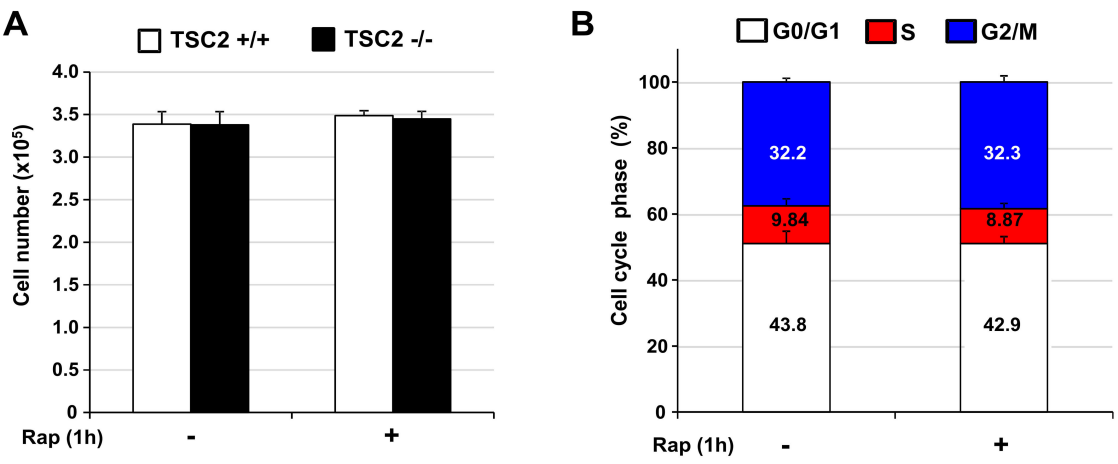

Fig. S1. Cell proliferation and cell cycle progression under the experimental conditions used to analyze steady state metabolites and metabolic flux in *Tsc2-/-* MEFs.

(**A**) *Tsc2*$^{+/+}$ and *Tsc2*$^{-/-}$ MEFs were serum starved for 15 h and were treated with vehicle (DMSO) or rapamycin (20 nM) for 1h, prior to viable cell counts.
(**B**) *Tsc2*$^{-/-}$ MEFs were treated as in (A), and cell cycle phases were quantified by FACS analyses.
Data are presented as mean±SEM over three independent samples per condition.

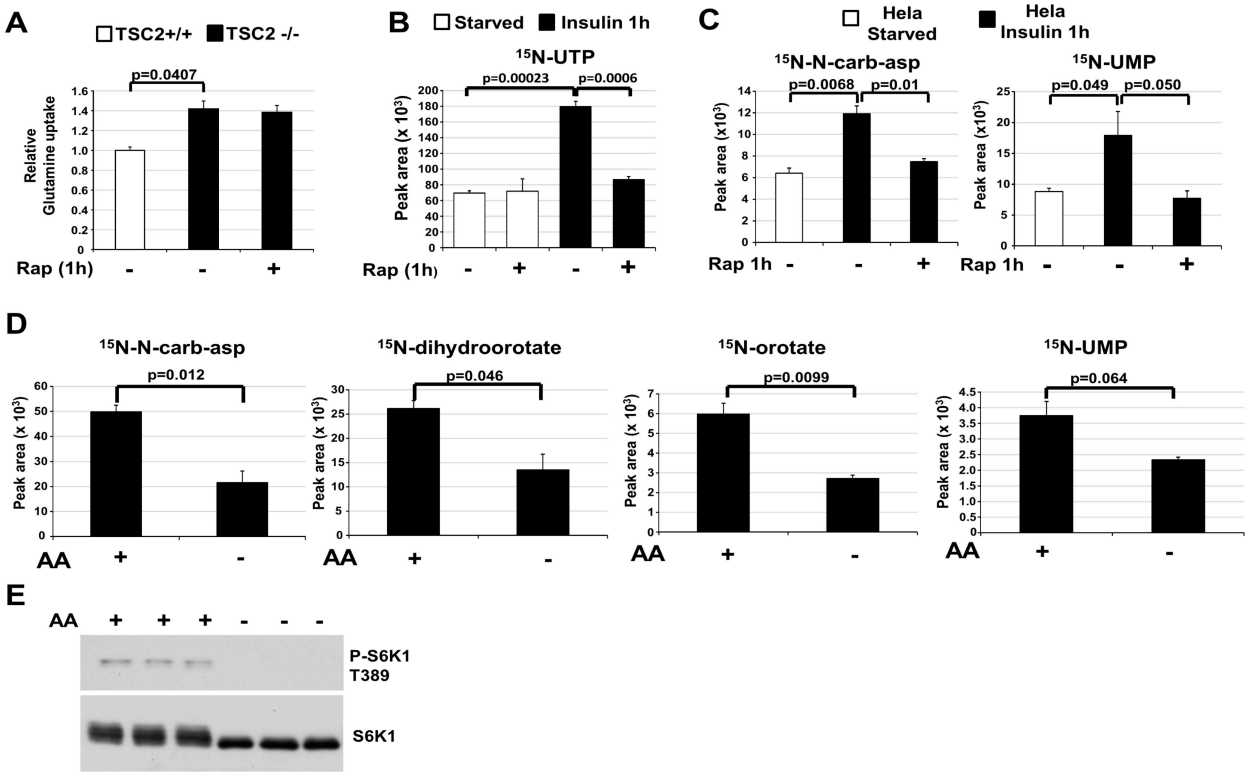

Fig. S2. Data supporting Fig 2.

(**A**) Glutamine uptake is not altered with 1 h treatment with rapamycin. *Tsc2*$^{+/+}$ and *Tsc2*$^{-/-}$ MEFs were serum starved for 15 h and treated with rapamycin (20 nM) for 1h. Glutamine uptake was measured as the incorporation of [U-^{14}C]-glutamine over 10 min and normalized to protein concentrations. Levels are presented as mean±SEM relative to *Tsc2*$^{+/+}$cells over three independent experiments.

(**B**) ^{15}N-labeled UTP levels from the ^{15}N-glutamine flux experiment in Fig. 2B are shown.

(**C**) An ^{15}N-glutamine flux experiment in HeLa cells, demonstrating that insulin-stimulated flux through pyrimidine synthesis is dependent on mTORC1. HeLa cells were serum starved for 15 h, treated with vehicle (DMSO) or rapamycin (20 nM) for 30 min, and then stimulated with insulin (100 nM) for 1h. Cells were incubated with ^{15}N-glutamine for 15 min immediately prior to metabolite extraction. Levels of ^{15}N-labeled pyrimidine pathway intermediates, measured via LC/MS/MS, are presented as mean±SEM over three independent samples per condition.

(**D**) An ^{15}N-glutamine flux experiment in wild-type MEFs, demonstrating that amino-acid starvation decreases flux through the pyrimidine synthesis pathway. Wild-type MEFs grown in dialyzed FBS (10%) were deprived of amino-acids for 2h. Cells were incubated with ^{15}N-glutamine for 15 min immediately prior to metabolite extraction. Levels of ^{15}N-labeled pyrimidine pathway intermediates, measured via LC/MS/MS, are presented as mean±SEM over three independent samples per condition.

(**E**) Immunoblots showing the inhibitory effects of amino acid starvation on mTORC1 signaling to S6K1 in parallel samples from (**D**).

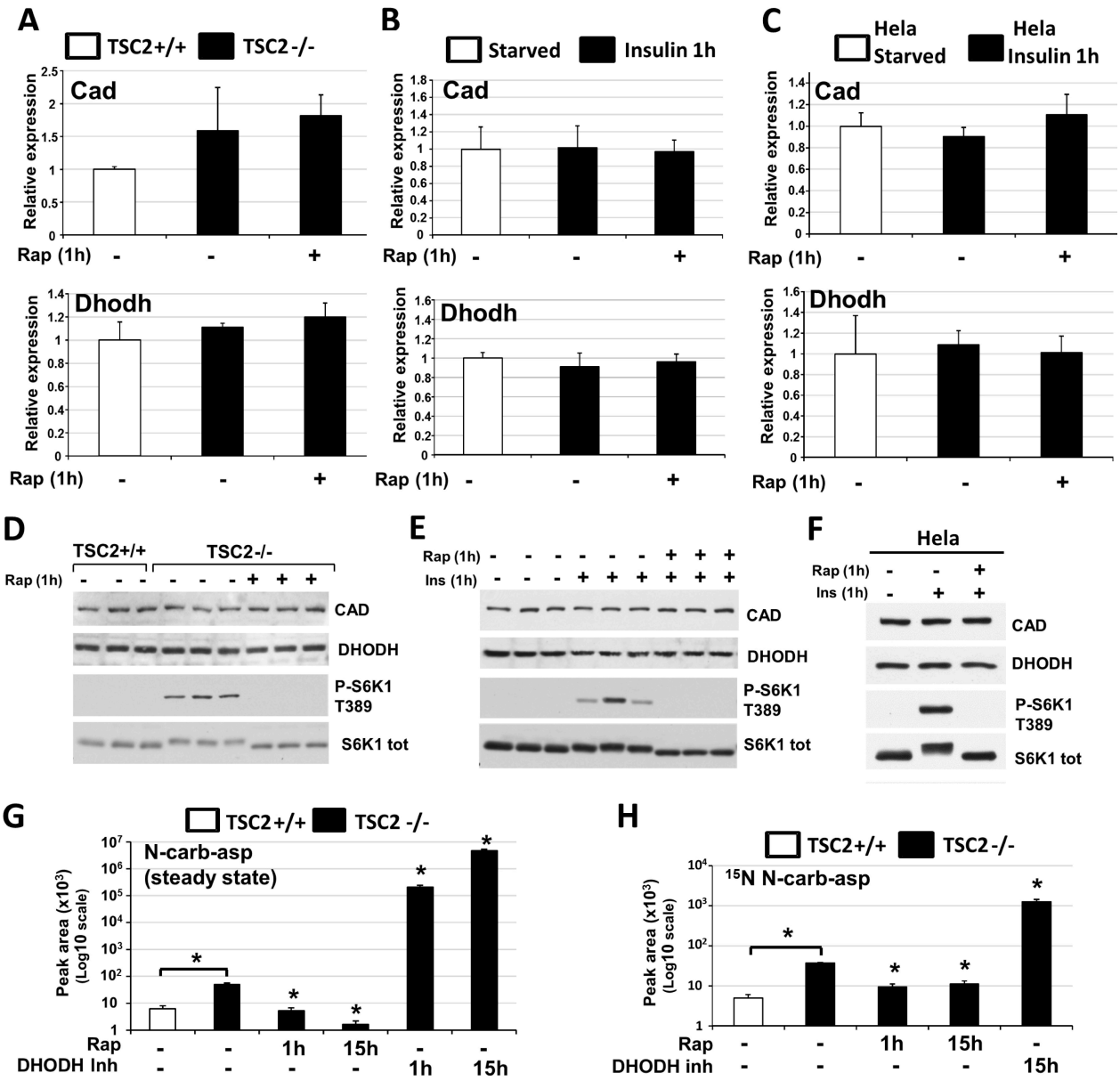
A
TSC2+/+
TSC2 -/-
Cad
Relative expression
Rap (1h) - - +
Dhodh
B
Starved
Insulin 1h
C
Hela Starved
Hela Insulin 1h
D
TSC2+/+
TSC2-/-
CAD
DHODH
P-S6K1 T389
S6K1 tot
E
Ins (1h)
F
Hela
G
N-carb-asp (steady state)
Peak area (x10³) (Log10 scale)
Rap
DHODH Inh
1h
15h
H
¹⁵N N-carb-asp
DHODH inh

Fig. S3. mTORC1 signaling affects N-carbamoyl-L-aspartate levels but not the mRNA or protein levels of CAD or DHODH.

(**A-C**) CAD and DHODH mRNA levels were measured by qRT-PCR and are presented as mean±SEM relative to untreated *Tsc2*$^{+/+}$ cells (**A**), unstimulated wild-type MEFs (**B**), or unstimulated HeLa cells (**C**).

(**D-F**) CAD and DHODH protein levels and mTORC1 signaling are shown in *Tsc2*$^{+/+}$ and *Tsc2*$^{-/-}$ MEFs (**D**), wild-type MEFs (**E**), and HeLa (**F**) under conditions of mTORC1 activation and inhibition. For (D) and (E), triplicate lysates are shown per condition.

(**A,D**) *Tsc2*$^{+/+}$ and *Tsc2*$^{-/-}$ MEFs were serum starved for 15 h and *Tsc2*$^{-/-}$ MEFs were treated with rapamycin (20 nM) for 1h.

(**B,E**) Wild-type MEFs were serum starved for 15 h and treated with vehicle (DMSO) or rapamycin (20 nM) for the final 15 min prior to 1 h stimulation with insulin (100 nM).

(**C,F**) HeLa cells were treated as described in (B,E).

(**G, H**) *Tsc2* $^{+/+}$ and *Tsc2*$^{-/-}$ MEFs were serum starved for 15 h in the presence of vehicle (DMSO), rapamycin (20 nM), or DHODH inhibitor (A771726, 10 μM) for either the final 1 h or the entire 15 h, prior to metabolite extraction. Relative steady state levels of N-carbamoyl-L-aspartate (**G**) or *de novo* synthesized ^{15}N-N-carbamoyl-L-aspartate, following ^{15}N-glutamine labeling for 15 min (**H**), were measured via LC/MS/MS. P-values for pairwise comparisons: (**G**): *Tsc2*$^{+/+}$ vs *Tsc2*$^{-/-}$ p=0.0044; *Tsc2*$^{-/-}$ vehicle vs 1 h rapamycin p=0.0038; *Tsc2*$^{-/-}$ vehicle vs 15 h rapamycin p=0.0026; *Tsc2*$^{-/-}$ vehicle vs 1 h DHODH inhibitor p=0.0065 ; *Tsc2*$^{-/-}$ vehicle vs 15 h DHODH inhibitor p=0.0008. (**H**): *Tsc2*$^{+/+}$ vs *Tsc2*$^{-/-}$ p=9x10^{-6}; *Tsc2*$^{-/-}$ vehicle vs 1 h rapamycin p=0.000042; *Tsc2*$^{-/-}$ vehicle vs 15 h rapamycin p=0.00013; *Tsc2*$^{-/-}$ vehicle vs 15 h DHODH inhibitor p=0.000016.

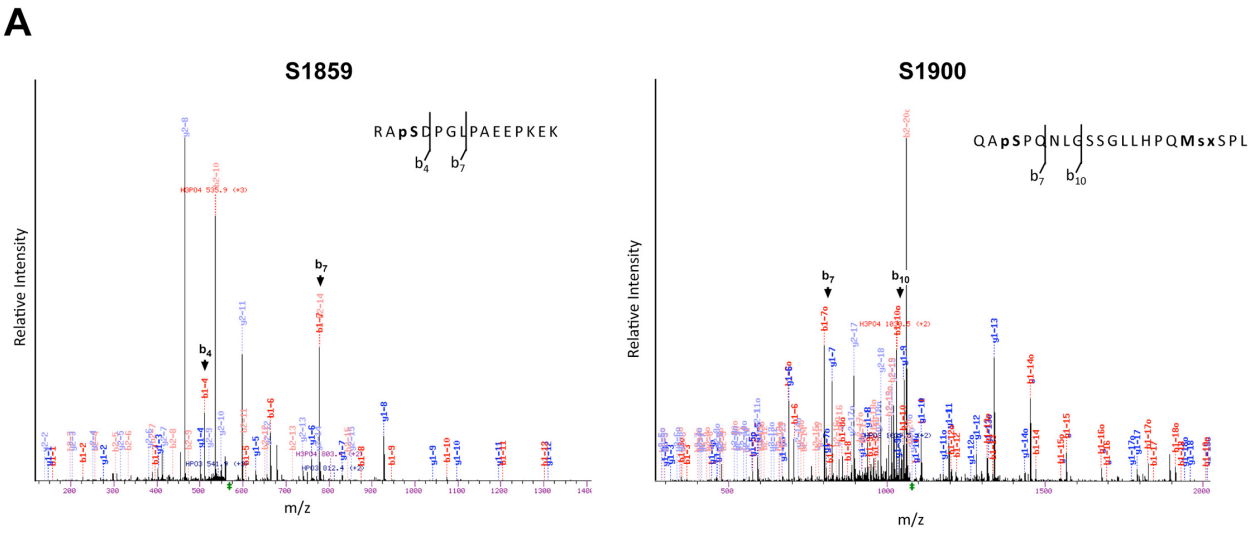
A
S1859
RApSDPGLPAEEPKEK
b4
b7
Relative Intensity
m/z
S1900
QApSPQNLGSSGLLHPQMsxSPL
b7
b10
Relative Intensity
m/z

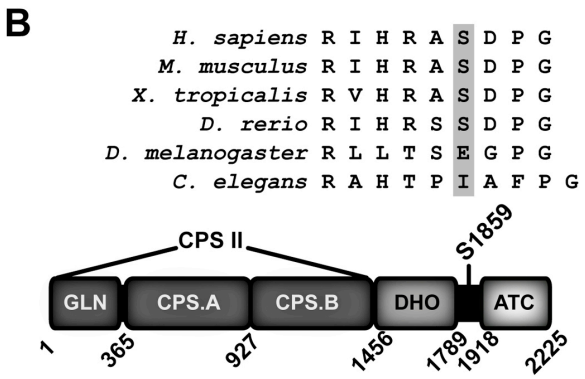
B
H. sapiens R I H R A S D P G
M. musculus R I H R A S D P G
X. tropicalis R V H R A S D P G
D. rerio R I H R S S D P G
D. melanogaster R L L T S E G P G
C. elegans R A H T P I A F P G
CPS II
S1859
GLN
CPS.A
CPS.B
DHO
ATC
1
365
927
1456
1789
1918
2225

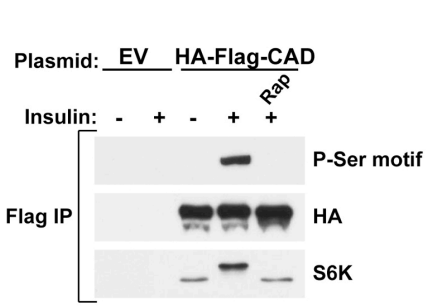
C
Plasmid: EV HA-Flag-CAD
Rap
Insulin: - + - + +
Flag IP
P-Ser motif
HA
S6K

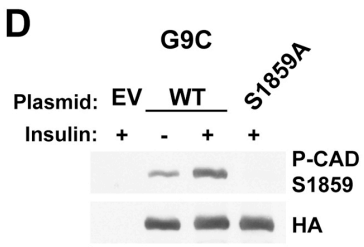
D
G9C
Plasmid: EV WT S1859A
Insulin: + - + +
P-CAD S1859
HA

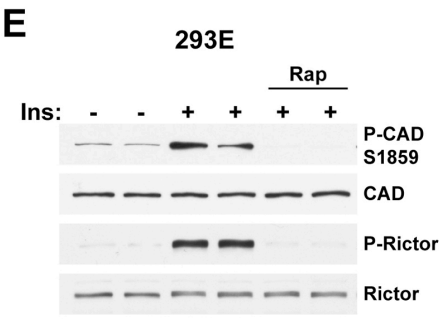
E
293E
Rap
Ins: - - + + + +
P-CAD S1859
CAD
P-Rictor
Rictor

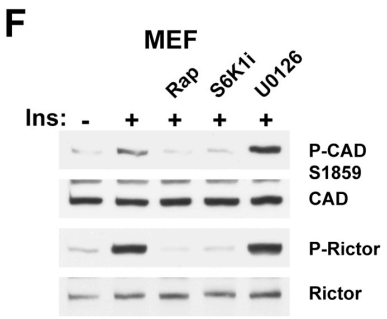
F
MEF
Rap
S6K1i
U0126
Ins: - + + + +
P-CAD S1859
CAD
P-Rictor
Rictor

Fig. S4. Identification of CAD phosphorylation sites and characterization of the S6K1-mediated phosphorylation of S1859 (supporting data for Fig 3).

(**A**) LC/MS/MS tandem mass spectrum for the triply charged peptide RApSDPGLPAEEPKEK (m/z 568.6) from CAD indicating a phosphorylation site at Ser3 on the peptide, corresponding to Ser1859 in the full length CAD protein. The prominent fragment ions b_4 and b_7 including a phosphate group identify the site as the N-terminal Ser residue as well as the triply charged neutral loss of phosphate (H_3PO_4) at m/z 535.9. Also shown (right) is the LC/MS/MS tandem mass spectrum for the doubly charged peptide QApSPQNLGSSGLLHPQMsxSPL (m/z 1079.5) from CAD indicating a phosphorylation site at Ser3 of the peptide, corresponding to Ser1900 in the full length CAD protein. The prominent fragment ions b_7 and b_{10} including a phosphate group identify the site as the N-terminal Ser residue as well as the doubly charged neutral loss of phosphate (H_3PO_4) at m/z 1030.5.
(**B**) Schematic showing the sequence conservation of S1859 among CAD orthologs and the location of S1859 in the linker region between the DHO (E3) and ATC (E2) domains on CAD.
(**C**) 293E cells transfected with FLAG-HA-CAD were serum starved overnight, pretreated for 1 h with vehicle (DMSO) or rapamycin (20 nM), followed by a 1 h stimulation with insulin (100 nM), where indicated. FLAG immunoprecipitates were immunoblotted with the indicated antibodies.
(**D**) G9C cells transfected with WT- or S1859A-CAD, were serum starved with or without 1 h stimulation with insulin (100 nM), and immunoblotted with a phospho-specific antibody to CAD-S1859 generated by Cell Signaling technologies (P-CAD S1859).
(**E**) 293E cells were serum starved (16 h) and pretreated for 30 min with vehicle or rapamycin prior to 1 h stimulation with insulin (100 nM), and immunoblotted as indicated.
(**F**) Wild-type MEFs were serum starved (16 h) and pretreated for 1 h with either rapamycin, S6K1i (10 μM), or the MEK inhibitor U0126 (10 μM) prior to 1 h stimulation with insulin (100 nM), and immunoblotted as indicated.

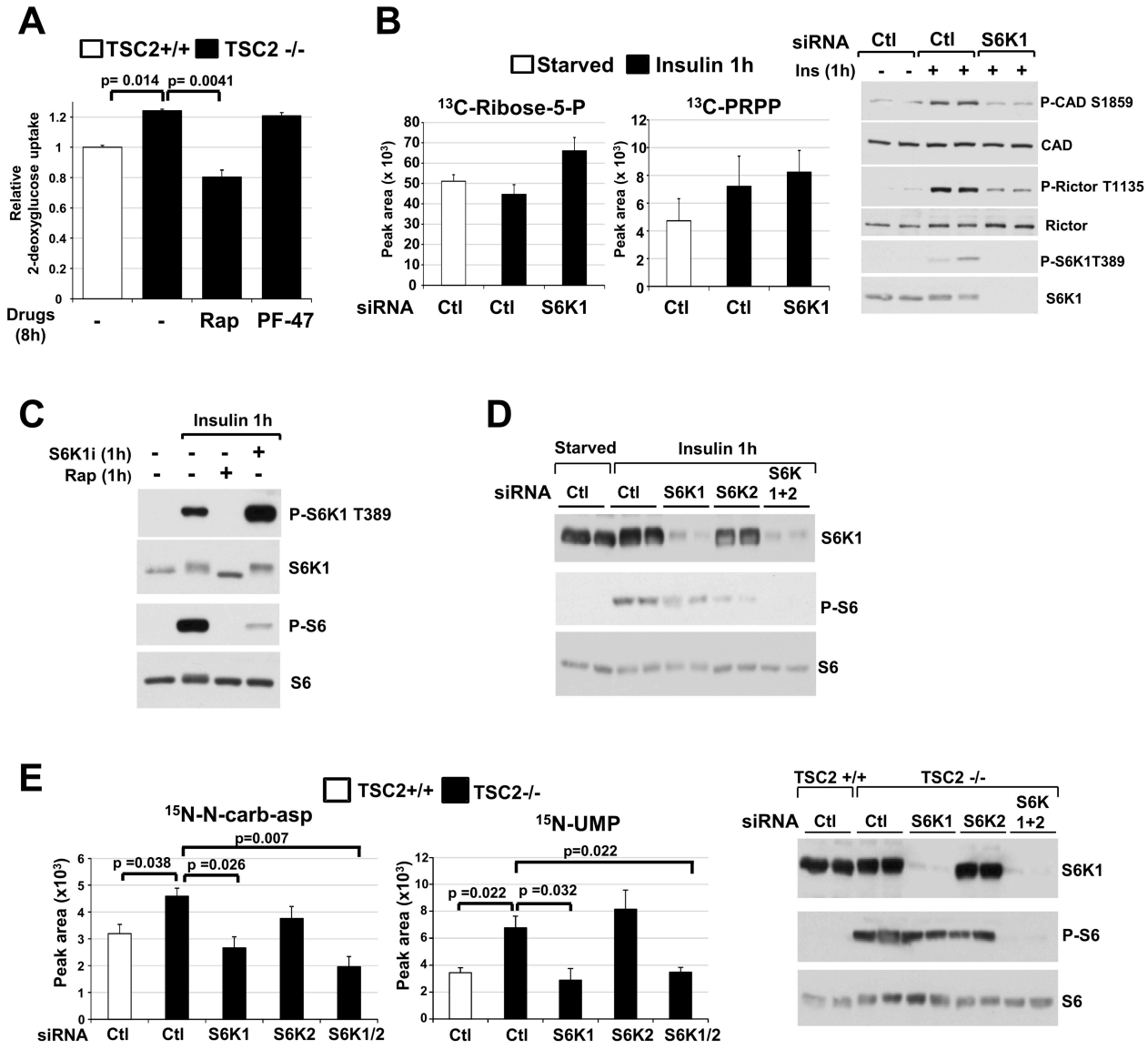
A
TSC2+/+
TSC2 -/-
p= 0.014
p= 0.0041
Relative 2-deoxyglucose uptake
Drugs (8h)
-
-
Rap
PF-47
B
Starved
Insulin 1h
13C-Ribose-5-P
13C-PRPP
Peak area (x 10³)
siRNA
Ctl
Ctl
S6K1
Ins (1h)
P-CAD S1859
CAD
P-Rictor T1135
Rictor
P-S6K1T389
S6K1
C
Insulin 1h
S6K1i (1h)
Rap (1h)
P-S6K1 T389
S6K1
P-S6
S6
D
Starved
Insulin 1h
siRNA
Ctl
Ctl
S6K1
S6K2
S6K 1+2
S6K1
P-S6
S6
E
TSC2+/+
TSC2-/-
15N-N-carb-asp
15N-UMP
Peak area (x10³)
p=0.007
p =0.038
p =0.026
p=0.022
p =0.022
p =0.032
siRNA
Ctl
Ctl
S6K1
S6K2
S6K1/2
TSC2 +/+
TSC2 -/-
S6K 1+2
S6K1
P-S6
S6

Fig. S5. Data supporting Fig 4.

(**A**) *Tsc2*$^{+/+}$ and *Tsc2*$^{-/-}$ MEFs were serum starved for 15 h and treated with either vehicle (DMSO), rapamycin (20 nM), or the S6K1 inhibitor PF-4708671 (PF-47, 10 μM) for 8h. Glucose uptake was measured as the incorporation of 1,2-^{3}H-2-deoxy-D-glucose over 5 min and normalized to protein concentrations. Levels are presented as mean±SEM relative to *Tsc2*$^{+/+}$ cells over three independent experiments. Significant p-values for *Tsc2*$^{+/+}$ versus *Tsc2*$^{-/-}$ and *Tsc2*$^{-/-}$ vehicle versus rapamycin are provided.

(**B**) Normalized peak areas of singly ^{13}C-labeled metabolites from the pentose phosphate pathway. WT MEFs were transfected with control (Ctl) or S6K1-directed siRNAs, and 48-h post-transfection were serum starved for 15 h and then stimulated by insulin (100 nM) for 1 h. Cells were pulse labeled for the final 15-min with [1,2-^{13}C]-glucose prior to metabolite extraction. Levels of singly ^{13}C-labeled pentose phosphate pathway intermediates, measured via LC/MS/MS, are presented as mean±SEM over three independent samples per condition. Immunoblots from parallel protein samples are provided to assess effects on S6K1 activity.

(**C, D**) Immunoblots supporting Fig 4A (**C**) and Fig 4B (**D**), and Fig 4C (**D**). Parallel samples to those described in Fig 4A and B were processed for immunoblotting.

(**E**) *Tsc2*$^{+/+}$ and *Tsc2*$^{-/-}$ MEFs were transfected with siRNAs targeting S6K1, S6K2, or both, or non-targeting controls (siCtl) for 48 h and serum starved for 15 h with ^{15}N-glutamine addition for the final 15 min prior to metabolite extraction. Levels of ^{15}N-labeled pyrimidine pathway intermediates, measured via LC/MS/MS, are presented as mean±SEM over three independent samples per condition. Immunoblots from parallel protein samples are provided to assess effects on S6K knockdown and activity.

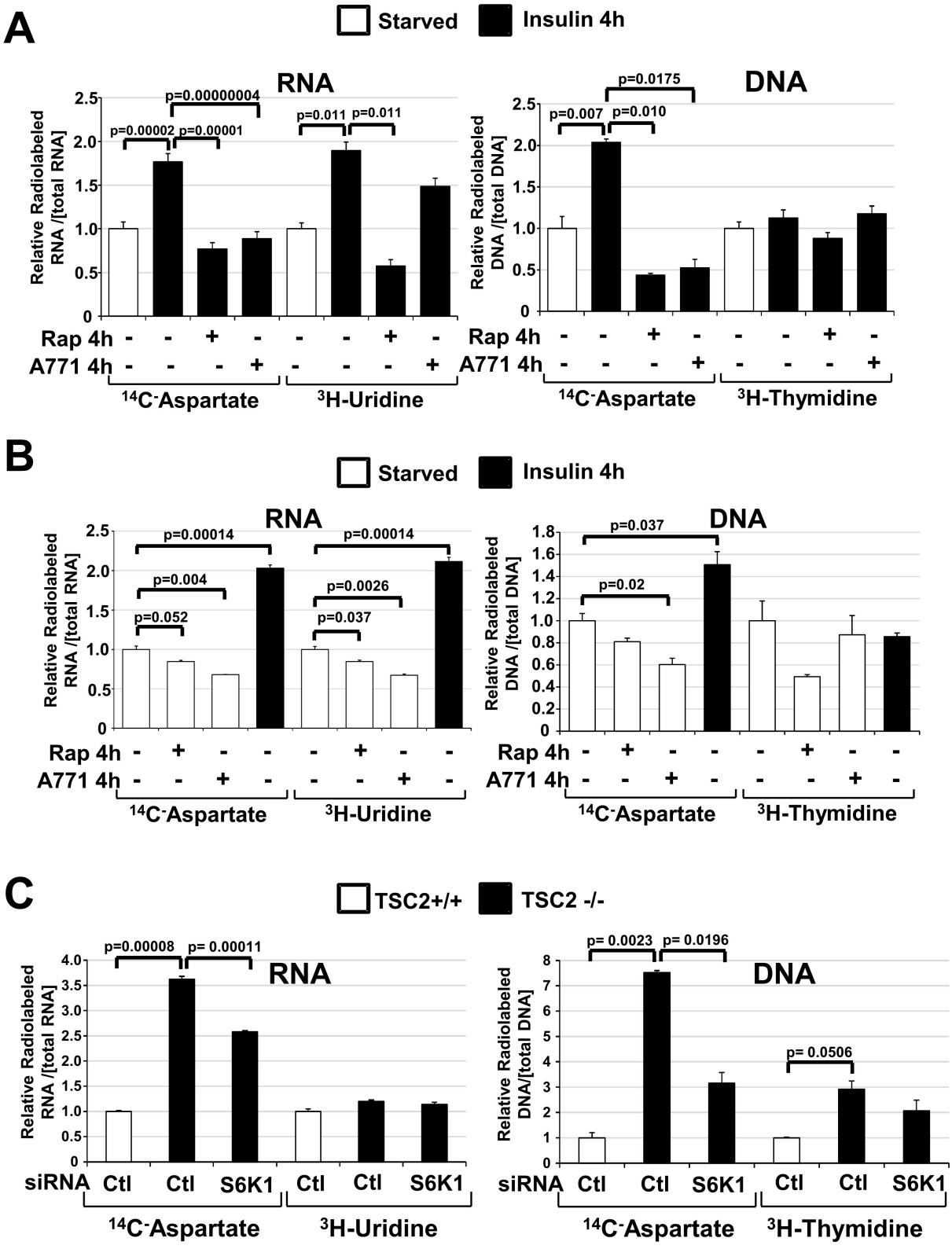
A
Starved
Insulin 4h
RNA
DNA
Relative Radiolabeled RNA /[total RNA]
Relative Radiolabeled DNA /[total DNA]
p=0.00000004
p=0.00002
p=0.00001
p=0.011
p=0.011
p=0.0175
p=0.007
p=0.010
Rap 4h
A771 4h
14C-Aspartate
3H-Uridine
3H-Thymidine
B
p=0.00014
p=0.00014
p=0.004
p=0.0026
p=0.052
p=0.037
p=0.037
p=0.02
C
TSC2+/+
TSC2 -/-
p=0.00008
p= 0.00011
p= 0.0023
p= 0.0196
p= 0.0506
siRNA
Ctl
S6K1

Fig. S6. S6K1 stimulates the incorporation of *de novo* synthesized pyrimidines into RNA and DNA.

(**A**) Wild-type MEFs were serum starved for 15 h and stimulated with insulin (100 nM) in presence or absence rapamycin (20 nM) or the DHODH inhibitor A771726 (A771, 10 μM) for 4h. Cells were labeled during this 4 h with either with [U-^{14}C]-aspartate, [5,6-^{3}H]-uridine, or [6-^{3}H]-Thymidine and incorporation of the specific radiolabel into RNA and DNA was measured and normalized to total concentration of RNA and DNA, respectively.

(**B**) Cells were treated and labeled as in (A), but the serum-starved cells were treated with the indicated inhibitors.

(**C**) *Tsc2*$^{+/+}$ and *Tsc2*$^{-/-}$ MEFs were transfected with the indicated siRNAs. 48 h postransfection, cells were serum starved for 15 h and labeled with either U-^{14}C-aspartate, [5,6-^{3}H]-uridine, or [6-^{3}H]-thymidine for 6h and incorporation of radiolabel into RNA and DNA was measured and normalized to total DNA and RNA concentrations.

All *P*-values≤ 0.05 for pairwise comparisons within these experiments are shown.

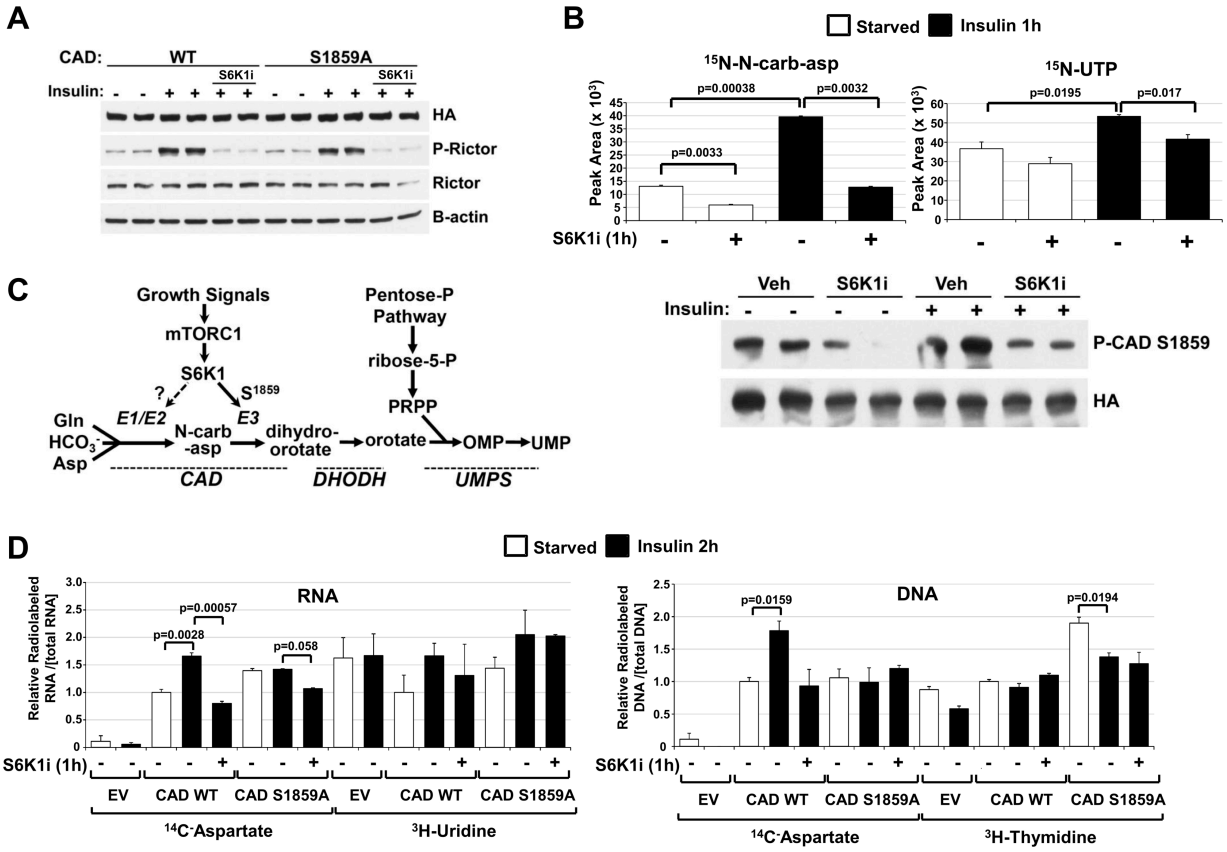
A
CAD:
WT
S1859A
S6K1i
Insulin:
HA
P-Rictor
Rictor
B-actin
B
Starved
Insulin 1h
15N-N-carb-asp
15N-UTP
Peak Area (x 10^3)
p=0.00038
p=0.0032
p=0.0033
p=0.0195
p=0.017
S6K1i (1h)
Veh
S6K1i
Insulin:
P-CAD S1859
HA
C
Growth Signals
mTORC1
S6K1
S1859
E1/E2
E3
Gln
HCO3-
Asp
N-carb
-asp
dihydro-
orotate
orotate
OMP
UMP
Pentose-P
Pathway
ribose-5-P
PRPP
CAD
DHODH
UMPS
D
Starved
Insulin 2h
RNA
Relative Radiolabeled
RNA /[total RNA]
p=0.00057
p=0.0028
p=0.058
S6K1i (1h)
EV
CAD WT
CAD S1859A
14C-Aspartate
3H-Uridine
DNA
Relative Radiolabeled
DNA /[total DNA]
p=0.0159
p=0.0194
3H-Thymidine

Fig. S7. Insulin- and S6K1-stimulated phosphorylation of CAD on S1859 promotes flux through the pyrimidine synthesis pathway into RNA and DNA.

(**A**) Immunoblots of parallel protein samples from G9C cells treated as in Fig. 4E, showing levels of HA-FLAG-CAD-WT and -S1859A and effects on S6K1 activity (P-Rictor).

(**B**) FLAG-HA-CAD-WT was transfected into CAD-deficient G9C cells, which were serum starved for 15 h and either left unstimulated or stimulated with insulin (100 nM) for 1 h in presence of vehicle (DMSO) or PF-4708671 (S6K1i, 10 μM). Cells were incubated with ^{15}N-glutamine for 15 min immediately prior to metabolite extraction. Levels of ^{15}N-labeled pyrimidine intermediates were measured and are presented as mean±SEM over three independent samples per condition accompanied with immunnoblots to assess CAD-S1859 phosphorylation.

(**C**) Model of mTORC1 signaling downstream of growth signals stimulating *de novo* pyrimidine synthesis through the S6K1-mediated phosphorylation of CAD-S1859, which metabolic flux analyses suggests affects the dihydoorotase (E3) activity of CAD. Data are also consistent with the possibility of additional, parallel inputs from S6K1 acting upstream of this activity.

(**D**) G9C cells stably expressing empty vector (EV), CAD-WT or CAD-S1859A were serum starved for 15 h, pretreated with vehicle or S6Ki (10 μM) for 1 h, and stimulated with insulin (100 nM) for 2h. Cells were labeled during this 2 h with either with [U-^{14}C]-aspartate, [5,6-^{3}H]-uridine, or [6-^{3}H]-Thymidine and incorporation of the specific radiolabel into RNA and DNA was measured and normalized to total concentration of RNA and DNA, respectively.

All *P*-values≤ 0.05 for pairwise comparisons within these experiments are shown.

Table S1 (separate excel file). LC/MS/MS peak areas and *P*-values for experiments described in Fig 1A-C (ranked by *P*-values of pairwise comparisons).

Table S2. SRM transitions of metabolites measured in the stable isotope-labeling flux experiments described in Fig 2, Fig 4, fig S2, fig S3, fig S5, and fig S7.

SRM for the pyrimidine biosynthesis pathway [^{15}N]-glutamine-amide		**Q1**	**Collision Energy (CE) (eV)**	**Q2**	
N-carbamoyl-L-aspartate	$C_5H_7N_2O_5^-$	175.03	11	132	
N-carbamoyl-L-aspartate_15N		176.03		133	
orotate	$C_5H_3N_2O_4^-$	155	13	111	$C_4H_3N_2O_2^-$
orotate_15N		156		112	
dihydroorotate	$C_5H_5N_2O_4^-$	157	12	113	$C_4H_5N_2O_2^-$
dihydroorotate_15N		158		114	
UMP	$C_9H_{14}N_2O_9P^+$	325	12	97	$C_5H_5O_2^+$
UMP_15N		326		97	
SRM for the pyrimidine biosynthesis pathway [4^{13}C]-L-aspartic acid		**Q1**	**Collision Energy (CE) (eV)**	**Q2**	
N-carbamoyl-L-aspartate-nega	$C_5H_7N_2O_5^-$	175.03	11	132	
N-carbamoyl-L-aspartate-nega_13C		176.03		133	
UMP	$C_9H_{14}N_2O_9P^+$	325	12	97	$C_5H_5O_2^+$
UMP_13C		326		97	
SRM for the pentose phosphate pathway [1,2^{13}C]-glucose		**Q1**	**Collision Energy (CE) (eV)**	**Q2**	
ribose-5-phosphate	C5H10O8P-	229	-35	79	PO3-
ribose-5-phosphate_13C1	C5H10O8P-	230	-35	79	PO3-
5-phosphoribosyl-1-pyrophosphate	C5H12O14P3-	389	-18	291	C5H9O10P2-
5-phosphoribosyl-1-pyrophosphate_13C1	C5H12O14P3-	390	-18	292	C5H9O10P2-

Table S3. *P*-values of pairwise comparisons for flux experiments in Fig 2.

A

p-values for flux analysis in Fig.2A

Metabolites	*Tsc2* $^{+/+}$ vs *Tsc2* $^{-/-}$	*Tsc2* $^{-/-}$ vs Rap
^{15}N-N-carbamoyl-L-aspartate	**0.00001**	**0.00004**
^{15}N-dihydroorotate	**0.04175**	**0.02417**
^{15}N-orotate	**0.03522**	**0.00366**
^{15}N-UMP	**0.00363**	0.34182

B

p-values for flux analysis in Fig.2B

Metabolites	Starved vs Rap	Starved vs Ins	Ins vs Ins + Rap
^{15}N-N-carbamoyl-L-aspartate	**0.26385**	**0.00700**	**0.02271**
^{15}N-dihydroorotate	**0.01373**	**0.00053**	**0.01194**
^{15}N-orotate	0.93371	**0.03514**	**0.02387**
^{15}N-UMP	0.95129	**0.02553**	0.05577

C

p-values for flux analysis in Fig.2C

Metabolites	*Tsc2* $^{+/+}$ vs *Tsc2* $^{-/-}$	*Tsc2* $^{-/-}$ vs Rap
^{13}C-N-carbamoyl-L-aspartate	**0.00319**	**0.04966**
^{13}C-UMP	**0.02384**	**0.00509**

D

p-values for flux analysis in Fig.2D

Metabolites	*Tsc2* $^{+/+}$ vs *Tsc2* $^{-/-}$	*Tsc2* $^{-/-}$ vs Rap 1h	*Tsc2* $^{-/-}$ vs Rap 15h
^{13}C-Ribose-5-P	**0.00009**	0.37766	**0.04618**
^{13}C-PRPP	**0.0000007**	0.13637	**0.00435**

Table S4. *P*-values of pairwise comparisons for experiments in Fig 4.

A

p-values for flux analysis in Fig.4A

Metabolites	Starved vs Ins	Ins 1h vs Ins + Rap	Ins 1h vs Ins + S6K1i
^{15}N-N-carbamoyl-L-aspartate	**0.00022**	**0.00017**	**0.00426**
^{15}N-UMP	**0.00155**	**0.02279**	**0.01167**

B

p-values for flux analysis in Fig.4B

Metabolites	Starved vs Ins siCtl	Ins siCtl vs Ins siS6K1	Ins siCtl vs Ins siS6K2	Ins siCtl vs Ins siS6K1+2
^{15}N-N-carbamoyl-L-aspartate	**0.00402**	**0.01155**	**0.04978**	**0.00452**
^{15}N-UMP	**0.02571**	0.06138	0.85126	**0.03178**

C

p-values for 14C or 3H incorporation into RNA/DNA in Fig.4C

RNA

Radiolabel	Starved vs Ins siCtl	Ins siCtl vs Ins siS6K1
[U-^{14}C]-L-aspartate	**0.00117**	**0.01899**
[5,6-^{3}H]-uridine	**0.00002**	0.27511

DNA

Radiolalabel	Starved vs Ins siCtl	Ins siCtl vs Ins siS6K1
[U-^{14}C]-L-aspartate	**0.03570**	**0.00293**
[5,6-^{3}H]-uridine	0.98124	0.83010

D

p-values for 14C or 3H incorporation into rRNA in Fig.4D

rRNA

Radiolabel	Starved vs Ins siCtl	Ins siCtl vs Ins siS6K1
[U-^{14}C]-L-aspartate	**0.03292**	**0.04194**
[5,6-^{3}H]-uridine	**0.03002**	0.44704

E

p-values for flux analysis in Fig.4E

Metabolites	CAD-wt Starved vs Ins	CAD-S1859A Starved vs Ins	CAD-wt Ins vs Ins +S6K1i	CAD-S1859A Ins vs Ins + S6K1i
^{15}N-N-carbamoyl-L-aspartate	**0.02859**	**0.00826**	**0.03887**	**0.00075**
^{15}N-Dihydroorotate	0.20007	0.60126	**0.01286**	0.78130
^{15}N-Orotate	**0.00715**	0.21696	**0.00812**	0.41889
^{15}N-UMP	**0.02634**	ND	ND	ND